

Cite this: *Chem. Commun.*, 2012, **48**, 3881–3883

www.rsc.org/chemcomm

## COMMUNICATION

**One-step synthesis of three-dimensional Pd polyhedron networks with enhanced electrocatalytic performance†**

You Xu, Rui Xu, Jianhua Cui, Yang Liu and Bin Zhang\*

Received 9th January 2012, Accepted 22nd February 2012

DOI: 10.1039/c2cc00154c

**Three-dimensional Pd polyhedron networks (Pd PNs) have been fabricated for the first time through a one-step, Cu<sup>2+</sup>-assisted, solution-chemical approach. These as-prepared 3D Pd PNs exhibit high stability and remarkably improved electrocatalytic activity toward formic acid oxidation over commercially available Pd black.**

Controlled synthesis of inorganic nanomaterials with well-defined morphologies and structures is considered to be a significant subject in the field of nanotechnology because the intrinsic properties of nanostructures strongly depend on their shape or surface atomic arrangement.<sup>1</sup> Surface defects on nanocrystals, such as step and kink atoms with low coordination numbers, usually exhibit very high chemical reactivity and catalytic activity toward most of the structure-sensitive reactions.<sup>2</sup> Constructing nanocrystals consisting of multitudinous surface defects through the fine-tuning of the exposure of the specific facets, corners, edges, and kinks is a promising approach to fabricate nanomaterials with high activity.

Palladium is extensively used in areas ranging from fuel cells, hydrogen storage, water treatment, hydrogen purification, as well as organic catalysis. Great efforts have been devoted to the preparation of various Pd nanocrystals, such as nanobars, nanorods, nanocubes, octahedra, icosahedra, and nanoplates.<sup>3</sup> Despite considerable investigation of morphological control of Pd nanocrystals, present studies have mainly focused on the monodisperse nanocrystals or some unstable assemblies. Using nanostructures as building blocks for the fabrication of multi-functional mesoscale architectures such as porous or network-like structure is an attractive approach to manufacture materials with new physical, chemical, and mechanical performance originated from their collective properties. However, to the best of our knowledge, there are limited studies which are aimed at the synthesis of Pd porous or network-like nanostructures composed of structural units such as nanowires,<sup>4</sup> nanoparticles,<sup>5</sup> and nanospheres.<sup>6</sup> Recently, we have developed a facile and robust synthetic strategy to fabricate noble metal

and alloy 3D networks by the synergism of interparticle electrostatic repulsion modulation and heat-induced fusion during nucleation and growth.<sup>7</sup> But, units in these 3D networks are composed of spherical particles. It remains untouched to develop a facile method to construct networks of Pd polyhedra, especially with high density of low-coordinated atomic steps.

Herein, three-dimensional (3D) Pd polyhedron networks (Pd PNs) have been prepared through a simple, one-pot, Cu<sup>2+</sup>-assisted, high yield solution-chemical method. These Pd PNs with 3D structure, high porosity, as well as interconnected network frames are composed of Pd polyhedra as building blocks. It is found that these 3D Pd PNs exhibit evidently enhanced catalytic activity and high stability for formic acid electrooxidation. This catalytic improvement may be associated with their intrinsic active sites including high density of atomic steps, ledges, and kinks, and stable network structure.

The typical synthesis procedure of 3D Pd PNs is described as follows: a mixture of 0.0446 mmol H<sub>2</sub>PdCl<sub>4</sub>, 0.0134 mmol Cu(NO<sub>3</sub>)<sub>2</sub>·2H<sub>2</sub>O, 20 mg dodecyl trimethylammonia bromide (DTAB), and 0.1 mL formaldehyde solution in 10 mL ethylene glycol (EG) was transferred into a 25 mL Teflon-lined stainless steel autoclave and heated at 150 °C for 8 h to obtain the products (see ESI† for details). The morphology and the structure of the as-obtained samples were firstly characterized by using scanning electron microscopy (SEM) and transmission electron microscopy (TEM). As shown in Fig. 1a, a representative low-magnification SEM image of the Pd samples suggests that

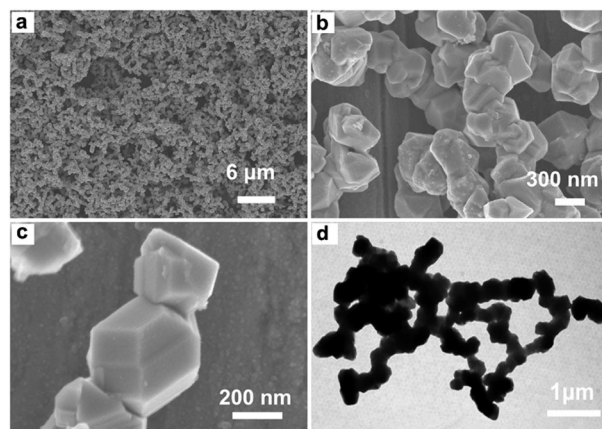


**Fig. 1** Low-magnification SEM image (a), high-magnification SEM images (b and c) and TEM image (d) of the 3D Pd PNs.

Department of Chemistry, School of Science, Tianjin University, Tianjin 300072, China. E-mail: bzhang@tju.edu.cn; Fax: +86 022 27403475; Tel: +86 022 27403475

† Electronic supplementary information (ESI) available: Experimental details, XRD patterns of the Pd NNs, SEM images of different Pd samples. See DOI: 10.1039/c2cc00154c

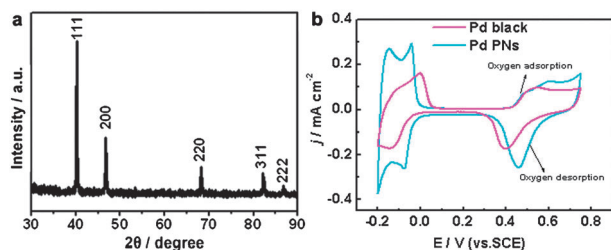


**Fig. 2** XRD pattern (a) of the Pd PNs and CV curves (b) of Pd PNs and Pd black in 0.1 M H<sub>2</sub>SO<sub>4</sub> solution at a scan rate of 0.05 V s<sup>-1</sup>. The current densities were normalized to the electrochemically active surface areas of the Pd catalysts.

three-dimensional porous network-like architectures were synthesized on a large scale. Upon closer examination through high-magnification SEM images (Fig. 1b and c), it can be distinctly seen that the 3D network-like architectures are constructed by numerous irregular polyhedra. Upon closer examination by TEM, the network structure was further confirmed, as evidenced in Fig. 1d. These polyhedra, as the building blocks of the network-like architectures, possess different morphology and size in a range from 200–400 nm.

To further examine the microstructure of the 3D Pd PNs, typical X-ray diffraction (XRD) pattern is recorded and presented in Fig. 2a. The diffraction peaks can be assigned to (111), (200), (220), (311), and (222) diffractions, respectively, which represents the typical character of a crystalline Pd face-centered cubic (fcc) phase (JCPDS 05-0681). Interestingly, no diffraction peaks from Cu or Cu oxide can be seen, which indicate that Pd samples with high crystallinity and purity were obtained.

Cu<sup>2+</sup> has been found to play a key role in the formation of the polyhedral nanocrystal building blocks. In the absence of Cu<sup>2+</sup> and other conditions kept unchanged, porous network structure consisting of irregular Pd nanoparticles with an average size of 50 nm, but not polyhedra, was produced (ESI†, Fig. S1). In fact, the amount of the copper ions introduced in the synthesis was important for the formation of the Pd polyhedron units. When the amount of Cu(NO<sub>3</sub>)<sub>2</sub> is 0.0134 mmol, the yield of the Pd polyhedra reaches nearly 100%. While the amount of Cu(NO<sub>3</sub>)<sub>2</sub> decreased to 0.009 mmol, although the network structure could be obtained, the polyhedral shape selectivity evidently decreased (ESI†, Fig. S2a). Also, when the amount of Cu(NO<sub>3</sub>)<sub>2</sub> was increased to 0.0178, 0.0268 and 0.0357 mmol, the yield of the polyhedra decreased along with the poor network structure generated (ESI†, Fig. S2b–S2d). These results suggest that the introduction of an appropriate amount of Cu(NO<sub>3</sub>)<sub>2</sub> would not only facilitate the formation of the Pd polyhedra, but also promote the generation of interconnected network structure. Copper ions have been used as the foreign ions in the synthesis of Pd and Pd-based alloy nanocrystals for shape control.<sup>8,9</sup> As reported in the Cu<sup>2+</sup>-assisted preparation of rod-like and branched palladium, some copper ions may be reduced and reoxidized during the second growth stage and serve as deposition or nucleation sites due to the relatively close reduction potential of Cu<sup>2+</sup>/Cu(0.34 V) with PdCl<sub>4</sub><sup>2-</sup>/Pd(0.61 V).<sup>8</sup> In our system, the reduction potential of palladium may be influenced by the surfactant (DTAB) existing in the reaction system, which makes their potential to be close. At appropriate concentration of copper ions, copper atoms preferentially deposit

at some specific sites, further reoxidize at varying instants and assist the next growth to polyhedra. The Cu<sup>2+</sup>-assisted growth mechanism can be also found to facilitate the formation of high-index facets in the synthesis of Au–Pd alloy nanocrystals.<sup>9</sup>

In our reaction system, formaldehyde is the main reducing agent, which can reduce PdCl<sub>4</sub><sup>2-</sup> to form Pd at 150 °C. The cationic surfactant, DTAB, can adsorb onto the as-formed nuclei or seeds when the metal precursors are reduced, and make these nuclei or seeds positively charged. As demonstrated in our previous work, the addition of EG is helpful to decrease the electrostatic repulsion of charged nuclei and seeds, and make  $V_{elec}$  (electrostatic repulsion potential) smaller than  $V_{vdw}$  (the van der Waals attraction potential) while still larger than half of  $V_{vdw}$ . This balance between  $V_{elec}$  and  $V_{vdw}$ , and the heated fusion will together lead to the formation of network-like structures.<sup>7</sup> Under such solvent-thermal conditions, the as-prepared Pd nanocrystals further form interconnected network structure instead of existing independently. Although the detailed mechanism how the Pd nanopolyhedra tend to connect together does still need further studies, the synergism of interparticle electrostatic repulsion modulation and heat-induced fusion during nucleation and growth may be responsible for this interesting phenomenon. By introducing a thermodynamic control of interparticle interactions and heat-induced interparticle fusion into the nucleation and Ostwald ripening process, 3D porous network structure can be fabricated.

Note that the relatively large size and stable 3D figure of Pd PNs make it very difficult to characterize the surface structure of Pd PNs using high-resolution transmission electron microscopy and selected electron diffraction. In order to further identify the surface structure of the 3D Pd PNs, electrochemical voltammetric methods were utilized to obtain overall structural information. The cyclic voltammogram (CV) of Pd PNs recorded in 0.1 M H<sub>2</sub>SO<sub>4</sub> solution at a scan rate of 0.05 V s<sup>-1</sup> at room temperature is presented in Fig. 2b, along with that of commercial Pd black (Aldrich) for comparison. The electrochemically active surface area (ECSA) of the Pd electrodes is calculated from the electric charges of reduction of monolayer Pd oxide with an assumption of 424 μC cm<sup>-2</sup> according to the CV curves.<sup>10</sup> The ECSAs were calculated to be 2.2 m<sup>2</sup> g<sup>-1</sup> for Pd PNs and 14.5 m<sup>2</sup> g<sup>-1</sup> for commercial Pd black. In comparison with commercial Pd black, the smaller ECSA of Pd PNs may be attributed to their larger building blocks (about 300 nm) than the Pd nanoparticles in Pd blacks. It is worth noting that the oxygen adsorption/desorption current on the Pd PNs is significantly larger than that observed on the polycrystalline Pd black catalyst as shown in Fig. 2b. Similar to oxygen adsorption on low-coordinated atomic steps of Pt,<sup>11</sup> more oxygen adsorption at low potential indicates that Pd PNs have high density of low-coordinated atomic steps<sup>12</sup> including high density of atomic steps, ledges, and kinks.

To evaluate the effect of the polyhedron-based network structure of 3D Pd PNs on their electro-catalytic properties, HCOOH oxidation on Pd PNs is selected as the probe reaction owing to the fact that HCOOH electrocatalysis on Pd is known to be structure sensitive.<sup>13</sup> For comparison, formic acid oxidation on commercially available Pd black is also tested. Fig. 3a displays the CVs of these two catalysts in 0.1 M HCOOH + 0.1 M H<sub>2</sub>SO<sub>4</sub>.

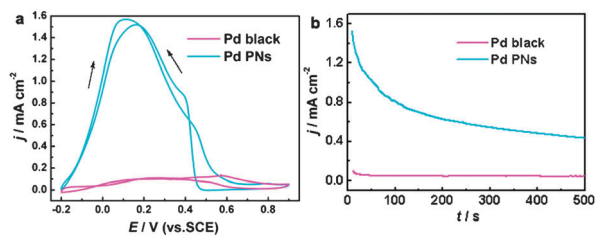


**Fig. 3** CV curves at a scan rate of  $0.05 \text{ V s}^{-1}$  (a) and chronoamperometric curves at  $0.1 \text{ V}$  (vs. SCE) (b) of Pd black and Pd PNs in  $0.1 \text{ M HCOOH} + 0.1 \text{ M H}_2\text{SO}_4$ . The currents were normalized to the ECSAs of Pd catalysts. The arrows in CVs (a) indicate the potential scan direction.

The currents are normalized to the ECSAs of the Pd catalysts. The forward peak current density for formic acid oxidation on Pd PNs is  $1.57 \text{ mA cm}^{-2}$ , which is about 12.1 times higher than that on Pd black ( $0.13 \text{ mA cm}^{-2}$ ). The currents were normalized to the mass amount of Pd catalysts to obtain the mass activities. The forward peak current density for formic acid oxidation on Pd PNs is  $27.5 \text{ mA mg}^{-1}$ , which is about 1.46 times higher than that on Pd black ( $18.8 \text{ mA mg}^{-1}$ ), as shown in Fig. S3a (ESI<sup>†</sup>). The higher current densities indicate that the Pd PNs exhibit enhanced electrocatalytic activity toward formic acid oxidation. The improved electroactivity of Pd PNs may be attributed to the effective electronic conduction through the high porosity and highly interconnected networks and the electronic states of the surface atoms because of the unique morphology of the 3D Pd networks and the exposure of their intrinsic active sites including high density of atomic steps, ledges, and kinks, and stable network structure.

The electrochemical stability of Pd PNs and commercially available Pd black on formic acid oxidation was studied by chronoamperometry. As presented in Fig. 3b and Fig. S3b (ESI<sup>†</sup>), a decrease in the current density with time is found in all these two catalysts, which can be attributed to the intermediate poisoning species formed from formic acid oxidation. Nevertheless, the current densities on the Pd PNs are evidently higher than those on Pd black over the entire time range, significantly confirming the better catalytic ability and stability of Pd PNs toward HCOOH oxidation than commercial Pd black.

In conclusion, 3D Pd PNs have been successfully prepared by a simple, one-pot,  $\text{Cu}^{2+}$ -assisted, solution-chemical synthesis method. The Pd PNs catalyst appears to exhibit high stability and remarkably improved catalytic activity for formic acid oxidation over commercially available Pd black, with promising applications in fuel cells and organic synthesis. Importantly, this synthesis method provides a new synthetic strategy to construct other noble metal or alloy polyhedron networks.

This work was financially supported by the National Natural Science Foundation of China (20901057 and 11074185) and the Tianjin Natural Science Foundation (10JCYBJC01800), Innovation Foundation of Tianjin University, and the Scientific Research Foundation for the Returned Overseas Chinese Scholars, State Education Ministry.

## Notes and references

- (a) E. Traebert, J. Clementson, P. Beiersdorfer, J. A. Santana and Y. Ishikawa, *Phys. Rev. A*, 2010, **82**, 062519; (b) C. Burda, X. Chen, R. Narayanan and M. A. El-Sayed, *Chem. Rev.*, 2005, **105**, 1025; (c) J. Watt, N. Young, S. Haigh, A. Kirkland and R. D. Tilley, *Adv. Mater.*, 2009, **21**, 2288; (d) S. Cheong, J. D. Watt and R. D. Tilley, *Nanoscale*, 2010, **2**, 2045; (e) Y. W. Lee, M. Kim, S. W. Kang and S. W. Han, *Angew. Chem., Int. Ed.*, 2011, **50**, 3466; (f) Y. Xia, Y. Xiong, B. Lim and S. E. Skrabalak, *Angew. Chem., Int. Ed.*, 2009, **48**, 60; (g) J. F. Li, Y. F. Huang, S. Duan, R. Pang, D. Y. Wu, B. Ren, X. Xu and Z. Q. Tian, *Phys. Chem. Chem. Phys.*, 2010, **12**, 2493; (h) J. Zhang, H. Yang, K. Yang, J. Fang, S. Zou, Z. Luo, H. Wang, I. T. Bae and D. Y. Jung, *Adv. Funct. Mater.*, 2010, **20**, 3727.
- (a) L. Dai and S. Zou, *J. Power Sources*, 2011, **196**, 9369; (b) S. W. Lee, S. Chen, W. C. Sheng, N. Yabuuchi, Y. T. Kim, T. Mitani, E. Vescovo and Y. Shao-Horn, *J. Am. Chem. Soc.*, 2009, **131**, 15669; (c) Q. N. Jiang, Z. Y. Jiang, L. Zhang, H. X. Lin, N. Yang, H. Li, D. Y. Liu, Z. X. Xie and Z. Q. Tian, *Nano Res.*, 2011, **4**, 612; (d) J. A. Santana, J. J. Mateo and Y. Ishikawa, *J. Phys. Chem. C*, 2010, **114**, 4995; (e) J. A. Santana and Y. Ishikawa, *Electrochim. Acta*, 2010, **56**, 945; (f) J. Watt, S. Cheong, M. F. Toney, B. Ingham, J. Cookson, P. T. Bishop and R. D. Tilley, *ACS Nano*, 2010, **4**, 396.
- (a) B. Lim, M. J. Jiang, J. Tao, P. H. C. Camargo, Y. M. Zhu and Y. N. Xia, *Adv. Funct. Mater.*, 2009, **19**, 189; (b) Y. J. Xiong, H. G. Cai, B. J. Wiley, J. G. Wang, M. J. Kim and Y. N. Xia, *J. Am. Chem. Soc.*, 2007, **129**, 3665.
- K. S. Krishna, C. S. Suchand Sandeep, R. Philip and M. Eswaramoorthy, *ACS Nano*, 2010, **4**, 2681.
- Z. Yin, H. J. Zheng, D. Ma and X. H. Bao, *J. Phys. Chem. C*, 2009, **113**, 1001.
- Y. Zhou, M. Kogiso and T. Shimizu, *J. Am. Chem. Soc.*, 2009, **131**, 2456.
- J. Cui, H. Zhang, Y. Yu, Y. Liu, Y. Tian and B. Zhang, *J. Mater. Chem.*, 2012, **22**, 349.
- Y. Chen, H. Hung and M. H. Huang, *J. Am. Chem. Soc.*, 2009, **131**, 9114.
- L. Zhang, J. Zhang, Q. Kuang, S. Xie, Z. Jiang, Z. Xie and L. Zheng, *J. Am. Chem. Soc.*, 2011, **133**, 17114.
- D. A. J. Rand and R. Woods, *J. Electroanal. Chem.*, 1971, **31**, 29.
- (a) N. Furuya and S. Koide, *Surf. Sci.*, 1989, **220**, 18; (b) Z. Zhou, Z. Huang, D. Chen, Q. Wang, N. Tian and S. Sun, *Angew. Chem., Int. Ed.*, 2010, **49**, 411; (c) N. Tian, Z. Zhou and S. Sun, *J. Phys. Chem. B*, 2008, **112**, 19801.
- (a) N. Tian, Z. Zhou and S. Sun, *Chem. Commun.*, 2009, 1502; (b) N. Tian, Z. Zhou, N. Yu, L. Wang and S. Sun, *J. Am. Chem. Soc.*, 2010, **132**, 7580.
- (a) N. Hoshi, K. Kida, M. Nakamura, M. Nakada and K. Osada, *J. Phys. Chem. B*, 2006, **110**, 12480; (b) N. Hoshi, M. Nakamura and K. Kida, *Electrochem. Commun.*, 2007, **9**, 279; (c) Z. L. Liu, L. Hong, M. P. Tham, T. H. Lim and H. X. Jiang, *J. Power Sources*, 2006, **161**, 831.